Anal. Bioanal. Electrochem., Vol. 12, No. 1, 2020, 48-62

Analytical & Bioanalytical Electrochemistry

Full Paper

Electrochemical Sensor for Selective Determination of Ketorolac Tromethamine based on Molecularly Imprinting Polypyrrole Modified with Functionalized Multi-wall Carbon Nanotubes in Pharmaceutical and Biological Samples

Azizollah Nezhadali* and Mohadese Biabani

Department of Chemistry, Payame Noor University, PO. Box 19395–4697, Tehran, Iran

*Corresponding Author, Tel.:+985138543357; Fax: +985138528520
E-Mail: aziz_nezhadali@Pnu.ac.ir

Received: 12 November 2019 / Accepted with minor revision: 15 January 2020 / Published online: 31 January 2020

Abstract- In this project, using a molecularly imprinting polypyrrole (MIP) modified with functionalized multi-wall carbon nanotubes (MWCNTs), a selective and sensitive electrochemical sensor constructed to measure ketorolac tromethamine (KT). Cyclic Voltammetry (CV), differential pulse Voltammetry (DPV) and chronoamperometry methods, respectively was performed in preparation of MIP, quantitative measurements and deposition of MWCNTs on the bare paper graphite electrode (PGE) surface. The nine factors were chosen for the investigation, which are: the concentration of MWCNTs, deposition time of MWCNTs onto the bare PGE surface, concentration of pyrrole, concentration of KT, number of cycles in electropolymerization, the pH of the polymerization solution, scan rate of CV process, electrode loading time, and stirring rate of loading solution. The multivariate methods, including Plackett-Burman design (PBD), and central composition design (CCD) were used for screening and optimizing of factors that could influence on the analytical response, respectively. Under the optimized conditions, the proposed MIP sensor showed a linear range from 4.0×10^{-6} to 6.0×10^{-3} M KT concentration with a correlation coefficient (R^2) of 0.9903. The limit of detection was obtained 0.12 µM ($3S_b/m$, n=6) with a highly reproducible response (RSD 4.45%, n=4). The electrochemical sensor showed good results for the determination of KT in pharmaceutical and biological samples.

Keywords- Polypyrrole, Ketorolac tromethamine, Molecularly imprinting polypyrrole, Multi-wall carbon nanotubes

1. INTRODUCTION

KT (Scheme 1) is a non-steroidal anti-inflammatory drug used in general anesthetics for the management of pain and inflammation associated with musculoskeletal [1,2]. Various analytical methods are described for the determination of KT in pharma clinical as well as biological fluids. These methods consist of non-aqueous titration, thin layer chromatography (TLC), ultraviolet-visible (UV) spectrophotometry [3,4], high performance liquid chromatography (HPLC) methods [5-8], solid-phase extraction [9] and electrochemistry [10,11]. Electrochemistry is a useful research tool for investigating drugs and pharmaceuticals that are electroactive. Varieties of techniques have been utilized: amperometry, conductometry, coulometry, ion-selective electrodes, potentiometry, stripping voltammetry (anodic and cathodic) and voltammetry. Analytical methods based on these techniques developed to monitor the quality of drugs manufactured as well as determining concentrations in physiological fluids for clinical applications [12].

One of the effective separation methods that have appeared in recent years is molecularly imprinting polymers (MIPs). MIP synthesized by simultaneous polymerization of functional and cross-linking monomers in the presence of the template molecule and used as a powerful, sensitive and selective absorber for the identification and measurement of the template molecule. MIPs have several advantages, including low cost, good physical and chemical stability, high selectivity and simplicity [13-19]. MIPs have been widely used in solid phase extraction [20], chromatographic separation [21], drug release [22], reaction catalysts [23], enzyme mimics [24], cancer biomarkers and viruses [25] and sensors [26,27]. Combining MIP with electrochemical methods was expected to result in an interesting new sensing technique [28, 29]. Polypyrrole (PPY) synthesized by electropolymerization technique [30-33]. The high adhesion of the polymer to the surface of the electrode and the control of the thickness of the polymer layer is one of the advantages of this technique [34]. The choice of electroactive functional monomers and fewer imprinted sites formed on the surface of an electrode are two major problems in the molecularly imprinted electropolymerization [35,36]. Monomers such as 3-acrylamidophenylboronic acid [37], and p-aminobenzenethiol phenol, aminophenyl boronate, phenylenediamine-co-aniline, phenylenediamine [38], pyrrole [34], aniline [39], o-aminophenol [40,41] are used to synthesize electrochemical MIPs, recently. In the past decade, the use of payrole was increasing because it is suitable in a natural pH range, and the resulting PPY film is easily made and has high chemical and electrochemical stability [42-45]. The second MIP problem is its low sensitivity and selectivity. By using functional nanomaterials, the intensity of the electrochemical signal increases, since the functional nanoparticles increase the electrode surface, conductivity, mass transport and ultimately improve the signal-to-noise ratio [46].

Electropolymerization method can be used to prepare MIP, but its disadvantages can be referred to them as low sensitivity of the sensor [47]. Increasing the thickness of the polymeric

layer will increase the molecular mold cavities, but the penetration of the molecule into the cavities will be slow [48].

Due to the unique properties of carbon nanotubes (CNTs), their use in chemical and biochemical sensors is increasing [49-51]. Good conductivity, tensile strength, low resistivity, the increase of the surface area, high chemical stability, ultra-small size, poor solubility and biocompatibility are unique properties of MWCNTs that increase the signal to noise ratio and increase the current sensor response [45].

Multivariate techniques for screening and optimization of the factors affecting the performance of polymer molecules and ultimately improve the sensitivity and selectivity it used to be [33,52]. Using the design of the experiment is a systematic, important and practical way to achieve optimal and valid results [53].

In this project, an electrochemical sensor was developed for the determination of KT. First, pyrrole electropolymerization carried out on the modified PGE surface in the presence of a KT and then, by removing the KT from the MIP holes, the sensor selected as a selective and sensitive micro-solid phase preconcentration sensor to the determination of KT, it was used in real samples.

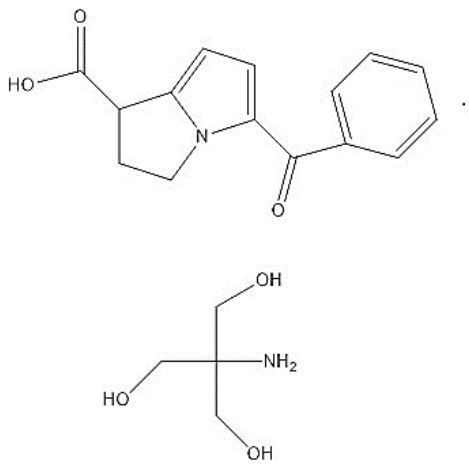

Scheme 1. Ketorolac teromethamine structure

2. EXPERIMENTAL

2.1. Chemicals and reagents

Sodium perchlorate monohydrate (99-102%), boric acid (99.9999 Suprapur), acetic acid (99.5%), pyrrole (≥97%) and Phosphoric acid (85%) were purchased from Merck (Darmstadt, Germany). Sodium hydroxide (98%) was purchased from Lobachemie (Mumbai, India). Ketorolac tromethamine was purchased from Sajad Darou Shargh Co. (Mashhad, Iran). MWCNTs (>95%) was purchased from Iranian Nanomaterials pioneers Co. (Mashhad, Iran).

2.2. Apparatus

The electrochemical studies done with a three-electrode system; a PGE (Owner, with 0.7 mm in diameter) modified with COOH-MWCNTs, a platinum wire and an Ag/AgCl (saturated KCl) as the working electrode, the counter electrode and the reference electrode, respectively. The voltammetric measurements carried out by Autolab PGSTAT 12 potentiostat–galvanostat (Ecochemie, The Netherlands). The surface evaluations of sensors performed by scanning electron microscopy (SEM) in an Oxford S360 SEM (Britain) microscope. The sonication of COOH-MWCNTs in deionized water was performed using a Hielscher ultrasonic bath processor (UTR200, Germany).

2.3. Hardware and software

In this project, a computer with 4 GB memory and an Intel Pentium 7.2.40 GHz CPU was used to experimental designs, statistical assessments and model fitting by the Minitab 16 software.

2.4. Fabrications of MIP/MWCNTs-COOH/PGE

First, for carboxylation of MWCNTs, 0.5 g of MWCNTs dissolved in 60 mL of concentrated nitric acid and refluxed at 100 °C for 12 h. The mixture was then passed through a filter and washed with deionized water until the pH of the resulting solution is neutral. The precipitate dried in vacuum and obtained the black functionalized carboxylic acid MWCNTs (MWCNTs-COOH) [54]. Second, the PGE was immersed in 6 M nitric acid for 15 minutes, then washed with distilled water and dried at room temperature. In order to modify the electrode with MWCNTs-COOH, the PGE was immersed in dispersed MWCNTs-COOH (0.36 gL^{-1} in distilled water) and the chronoamperometric technique with the potential of 1.7 V for 336 seconds was used. After drying at room temperature, the modified PGE as a working electrode was immersed in 15 mL of polymerization solution (0.07 M pyrrole, 0.002 M KT and 0.1 M $NaClO_4$ in Britton-Robinson (BR) buffer solution (0.04 M H_3PO_4/0.04 M H_3BO_3/0.04 M CH_3COOH, adjusted in pH 4)). Then PPY film obtained by applying cyclic voltammetry (CV) technique between -1.00 V to 2.00 V for 12 cycles. To remove the KT from the holes of imprinting polymer, differential pulse voltammetry (DPV) technique was used in the range of 0.75 V to 0.95 V in BR buffer solution adjusted in pH 4, so that no oxidation peak was observed for the KT. For non-imprinted polymer (NIP) preparation, Polymerization was carried out in the absence of KT.

2.5. Electroanalytical measurements

The voltammetric measurements were done in a three-electrode system in BR buffer at pH 4. DPV runs were recorded from 0.75 V to 0.95 V at the scan rate of 8.0 mV/S, applying step potential of 0.00405 V and modulation amplitude of 0.4995 V, at room temperature.

2.6. Sample preparation

In order to evaluate the accuracy of the proposed method, 0.5 mL human blood serum, prepared from a local medical clinic, was spiked with a KT standard solution to give a working concentration of KT (0, 20, 40 and 60 μM). This sample was placed into a 1.5 Eppendorf Safe-Lock micro centrifuge tubes, including 0.5 mL of acetonitrile and diluted to 1.5 mL with deionized water. Then, vortexes for 10 s and centrifuged at 2500 r.p.m. for 25 min to eliminate serum protein and 0.5 ml of clear solution was transferred into a volumetric flask and fixed to 10 ml using deionized water [55].

In addition, KT was determined in a tablet sample pharmaceutical (Sajad Darou Shargh). Four tablets of each brand weighed and powdered. Then the average weight of the tablets from the powder was dissolved in deionized water. The mixture was then filtered and the resulting solution was transferred to a 10 ml volumetric flask and reached the volume of 10 mL and spiked with a standard solution of KT at different concentrations. For the preparation of ampoule sample, 0.1 mL of ampoule sample (Alborz Darou) dilute to 10 mL with deionized water and spiked with a standard solution of KT at different concentrations and used for analysis.

3. RESULTS AND DISCUSSION

Following pyrrole electrooxidation at the surface of MWCNTs-PGE, as an anode, a PPY black deposit form on its surface. In the interaction between monomer pyrrole and KT molecules, KT is trapped in the conductive polymeric matrix and the sensitive and selective cavities are obtained by evacuation of the KT [18]. Cyclic voltammogram of MIP and NIP is has been shown in Figure 1. Due to the interaction between KT and monomer pyrrole, there is a clear peak in Figure 1A, which is not shown in Figure 1B.

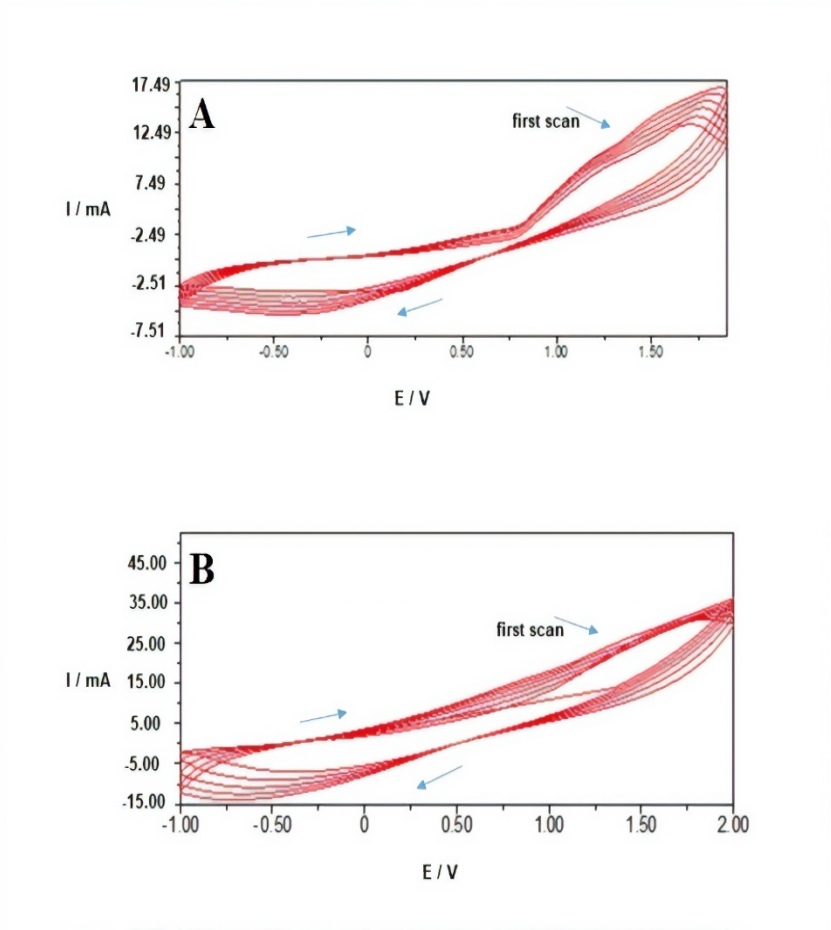

Fig. 1. The voltammetric cycles for the preparation A: MIPs/MWCNTs-COOH/PGE and B: NIPs/MWCNTs-COOH/PGE, in a BR buffer with pH 4, 0.1 M $NaClO_4$, 0.07 M pyrrole and 0.002 M KT

3.1. Experimental design

3.1.1. Screening of significant factors

To maximize the amount and accuracy of information that was received from a given set of experimental runs, a planned sequence of experiments linking changes in input variables with changes in MIP voltammetric response was designed. This experimental design facilitated the study of how responses change and interact at different variable settings. The Plackett-Burman (PB) design, as a great value in screening experiments, identifies the effective factors and reduces the number of runs [34,56]. According to previous work, nine factors were chosen for the investigation, which are: the concentration of MWCNTs(A), deposition time of MWCNTs onto the bare PGE surface (B), concentration of pyrrole (C), concentration of KT (D), number of cycles in electropolymerization (E), pH of the polymerization solution (F), scan rate of CV process (G), electrode loading time (H) and stirring rate of loading solution (J). A low and high level was considered for each of the variables. A PB design was carried out for

nine factors, consisting of 12 randomized runs. Table 1 shows the experimental results for the 12-run PB design.

Table 1. The results of PB experimental design matrix

Run Order	A	B	C	D	E	F	G	H	J	I_{MIP} (µA)	$I_{MIP-NIP}$ (µA)
1	0.36	400	0.07	0.002	5	4	100	15	400	2.8	2.61
2	0.36	1200	0.01	0.005	5	4	50	15	400	0.57	0.43
3	0.20	1200	0.07	0.002	10	4	50	5	400	0.86	0.60
4	0.36	400	0.07	0.005	5	7	50	5	100	0.15	-0.30
5	0.36	1200	0.01	0.005	10	4	100	5	100	0.63	0.54
6	0.36	1200	0.07	0.002	10	7	50	15	100	0.70	0.69
7	0.20	1200	0.07	0.005	5	7	100	5	400	0.24	-0.43
8	0.20	400	0.07	0.005	10	4	100	15	100	2.41	2.31
9	0.20	400	0.01	0.005	10	7	50	15	400	1.95	0.71
10	0.36	400	0.01	0.002	10	7	100	5	400	2.46	2.27
11	0.20	1200	0.01	0.002	5	7	100	15	100	1.47	-0.47
12	0.20	400	0.01	0.002	10	4	50	5	100	1.49	-0.34

Figure 2A and B illustrates the standardized Pareto plot of the main effects for PB design and main effect plot for voltammetric response at 95% confidence level ($p \leq 0.05$), respectively. The Pareto plot shows that effects of B, E and G factors are most important to the process. The main effects plot for voltammetric response shows the effective level of each factor. Therefore, B factor in low level and E and G factors in the high level have more impact on the experiment and need to be optimized more accurately.

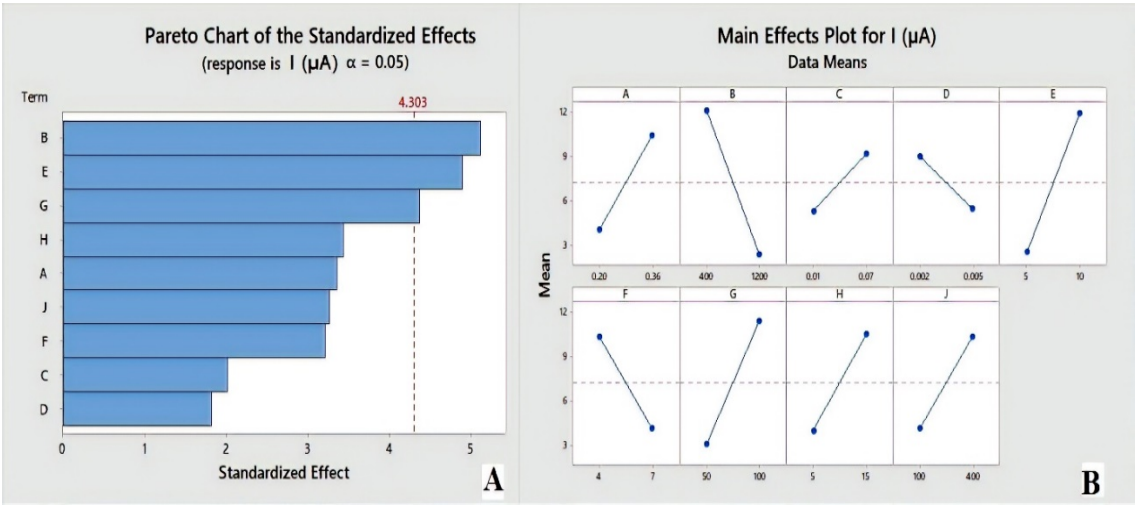

Fig. 2. A: The main effect pareto chart for PB design and B: The main effects plot for voltammetric response

3.1.2. Optimization

Central composite design (CCD) is a simple and useful design that used to optimize a wide range of empirical effective factors [57]. A three-level CCD with 20 runs was carried out for optimization of the process after screening by PB design. The results are shown in Table 2 for each experiment the voltammetric runs were obtained on MIP and NIP sensor under the identical operating condition and the difference between MIP and NIP sensor voltammetric response has been mentioned for each run.

Table 2. The CCD matrix and the experimental results

Run Order	B	G	E	I_{MIP} (µA)	I_{MIP_NIP} (µA)
1	300	70	8	2.36	1.33
2	500	70	8	4.71	4.28
3	300	130	8	1.92	1.22
4	500	130	8	8.16	7.50
5	300	70	12	12.34	10.12
6	500	70	12	7.14	3.07
7	300	130	12	7.63	6.91
8	500	130	12	2.93	2.77
9	400	100	10	7.12	6.63
10	400	100	10	6.85	6.16
11	400	100	10	7.46	6.53
12	400	100	10	6.74	6.22
13	300	100	10	3.93	3.68
14	500	100	10	6.37	3.74
15	400	70	10	7.40	6.36
16	400	130	10	8.63	7.01
17	400	100	8	6.12	5.91
18	400	100	12	9.34	8.67
19	400	100	10	7.51	6.63
20	400	100	10	7.85	6.77

The aim of this analysis is to increase the difference between MIP and NIP sensor voltammetric response. The following equation was obtained based on the regression analysis:

$$I_{MIP\text{-}NIP}=-76.27+0.3237B-0.0041G+3.149E-0.000280B*B+0.000194G*G+0.1950E*E+0.000260B*G-0.012762\ B*E-0.01379\ G*E$$

Using analysis of variance (ANOVA), presented in Table 3, the validation of the statistical result was analyzed. R^2 and R^2_{adj} for models were obtained 99.20% and 98.48% ($p\leq0.05$), respectively. The lack of fit p-value was obtained 0.278. According to the response surface optimization, the optimal conditions were obtained 336 s, 70 mVs^{-1} and 12 for B, G and E factors, respectively.

Table 3. The ANOVA results for evaluation of mathematical models obtained by response surface design

Source	DF[a]	Adj SS[b]	Adj MS[c]	F-value	P-value
Linear	3	13.136	4.3787	52.97	0.000
Square	3	27.170	9.0567	109.56	0.000
Interaction	3	62.467	20.8224	251.90	0.000
Lack-of-Fit	5	0.526	0.1051	1.75	0.278
Pure error	5	0.301	0.0602		
Total	19	103.600			

a: Degrees of freedom
b: Adjusted sum of squares
c: Adjusted mean squares

3.2. Surface characterization

The morphological structures of the PGE bare (Figure 3A), MWCNTs-COOH/PGE (Figure 3B), NIP/ MWCNTs-COOH/PGE (Figure 3C) and MIP/ MWCNTs-COOH/PGE (Figure 3D) were investigated by scanning electron microscopy (SEM).

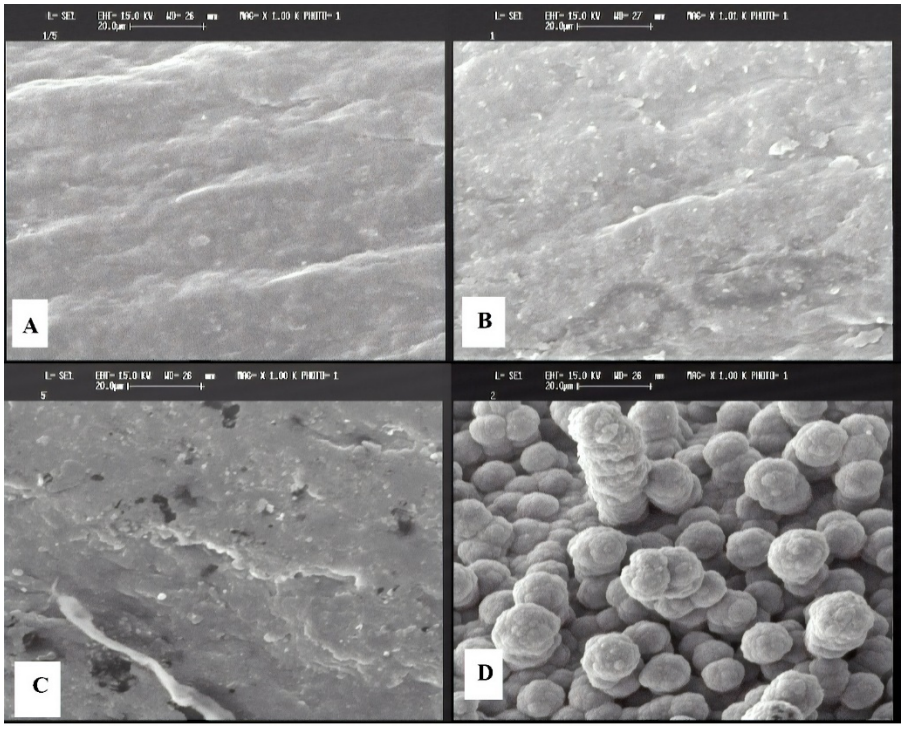

Fig. 3. The surface morphology of A: PGE bare; B: MWCNTs-COOH/PGE; C: NIP/MWCNTs-COOH/PGE and D: MIP/MWCNTs-COOH/PGE

SEM images show a uniform surface of MWCNTs-COOH that were distributed on the electrode surface (Figure 3A and B). SEM image shows a uniform film of MIP was distributed

on the electrode surface (Figure 3D). After immobilization of MIP polymer on the surface of MWCNTs-COOH/PGE, the SEM image of the resulted electrode demonstrate the significant morphological difference between MWCNTs-COOH/PGE and MIP/MWCNTs-COOH/PGE, respectively. The Polymerization conditions, such as the type of supporting electrolyte, polymerization solvent etc. are effective on electropolymerized PPY [58]. The SEM imaging of MIP clearly shows an irregular morphology on the surface of the MIP/MWCNTs-COOH/PGE, that facilitates the fast binding of template molecules to the polymer [59]. The surface of MIP/MWCNTs-COOH/PGE exhibits more porous than the one of NIP/MWCNTs-COOH/PGE (Figure 3C and D). The presence of the KT in the polymerization solution causes the formation of holes in the MIP film and changes the morphology of the polymer [52].

3.3. Figures of merit

In order to investigate the dependence of the voltammetric response of the proposed sensor on the concentration of KT, different concentrations of KT in optimal conditions were measured by the proposed MIP sensor. The calibration curve showed a dynamic linear range from 4.0×10^{-6} to 6.0×10^{-3} M KT (Figure 4A and B), with a linear regression equation:

$$I_{MIP} = 3.6431 + 3656.5\ C_{KT}$$

where, C_{KT} is KT concentration and, I_{MIP} is the voltammetric anodic peak current of MIP (μA). The correlation coefficient is 0.9903.

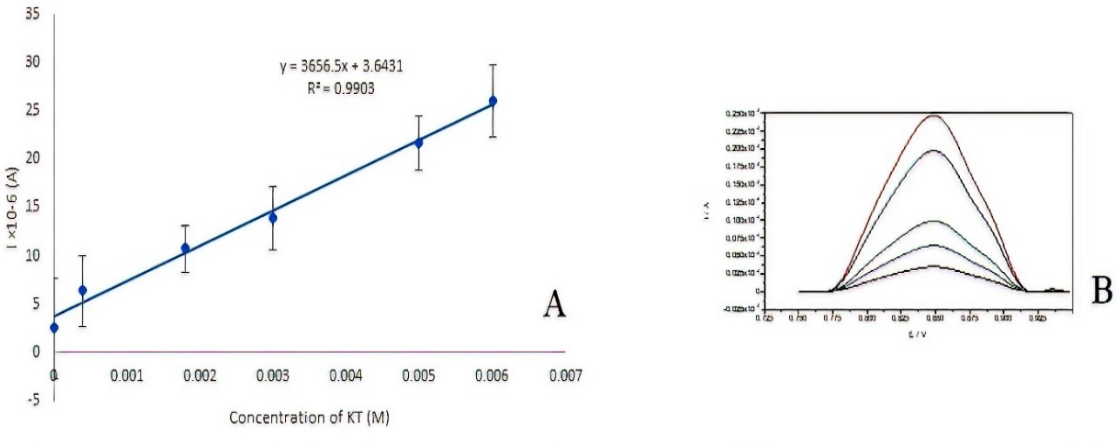

Fig. 4. A: The calibration curve of KT and B: The differential pulse voltammograms for different concentrations of KT

The detection limit of KT was obtained 0.12 μM ($3S_b/m$, n=6). The repeatability of MIPs/MWCNTs-COOH/PGE was investigated and the peak current response of KT was

determined using the same electrode. The results showed a RSD of 4.45%, confirming that the prepared sensor was repeatable after four times used. Inter day stability of the sensor was investigated and the current response was measured, the current was unaltered and a decrease of 29.26% in the current response occurred after the 20th day. Compared to other analytical methods, the proposed method has a low detection limit and the wider linear range to determine of KT (Table 4) [1,60-62].

Table 4. The comparison of the results of different techniques on determination of KT

Technique	Detection method	Linear rang (µM)	LOD (µM)	Ref.
Isocratic HPLC	UV	132.8-398.5	308.1	[1]
Direct oxidation	UV	16.6-99.6	4.9	[60]
Reverse phase HPLC	UV	0.5-26.5	1.3	[61]
Electrochemistry	DPV	10-350	0.08	[62]
MIP	DPV	4.0-6×10^3	0.12	This work

Table 5. The selectivity of sensor KT (10^{-4} M) in presence of interfering molecules (n=3)

Interfere molecule	KT: Interfere molecule	Change in current response for detection of 10^{-4} M KT	Recovery (%)
Chloroquine phosphate	1:1	-0.261	92.65
	1:2	-0.002	99.41
	1:4	+0.260	107.31
Captopril	1:1	-0.100	97.19
	1:2	-0.234	93.43
	1:4	+0.098	102.77
Para-aminobenzoic acid	1:1	+0.039	101.10
	1:2	-0.309	91.33
	1:4	-0.338	90.51
Simvastatin	1:1	-0.462	87.02
	1:2	-0.322	90.96
	1:4	-0.257	92.79
Rabeprazole	1:1	-0.230	93.54
	1:2	-0.328	90.80
	1:4	-0.421	88.16
Fluvoxamine	1:1	-0.133	96.27
	1:2	-0.224	93.72
	1:4	+0.082	102.09

3.4. Selectivity of MIP/MWCNTs-COOH/PGE

In order to evaluate the proposed sensor selectivity, the KT oxidation peak was investigated for the solution containing 1×10^{-4} M KT and different concentration of each interferes like chloroquine phosphate, captopril, para-aminobenzoic acid, simvastatin, rabeprazole and

fluvoxamine. Table 5 shows the results of measurement of KT in the presence of interferes. The results confirm the selectivity of the MIP sensor for the KT relative to interfering substances.

3.5. Analysis of real samples

Table 6 shows the results of measurement of KT in human blood serum and pharmaceutical samples. Each analysis repeated three times under the optimized conditions and the results are satisfactory.

Table 6. The result of KT determination in real sample analysis (n=3)

Sample	KT added (µM)	average of KT found (µM) ± RSD[a]	Recovery (%)
Serum	0	Not detected	-
	20	19.44±1.41	97.20
	40	39.25±2.05	98.13
	60	58.98±1.13	98.28
Ampoule[b]	0	26.60±3.21	-
	20	46.20±0.43	99.14
	40	65.74±2.52	98.71
	60	86.17±1.03	99.50
Tablet[c]	0	26.64±3.11	-
	20	46.02±4.02	98.67
	40	65.83±2.71	98.78
	60	84.68±1.92	97.74

a: Ralative Standard Deviation
b: Alborz darou Co.
c: Sajad darou shargh Co

4. CONCLUSION

In this project, an electrochemical sensor was developed for the determination of KT. First, pyrrole electropolymerization carried out on the modified PGE surface in the presence of a KT and then, by removing the KT from the MIP holes, the sensor selected as a selective and sensitive micro-solid phase preconcentration sensor to the determination of KT, it was used in standard solutions, human blood serum and pharmaceutical samples. Screening of effective factors and their optimization were performed with multivariate optimization methods. Under the optimal conditions, the electrochemical sensor showed a good result in the determination of KT in a linear range from 4.0×10^{-6} to 6×10^{-3} M, with a detection limit of 0.12 µM (3sb/m, n=6).

REFERENCES

[1] G. Sunil, M. Jambulingam, S. A. Thangadurai, D. Kamalakannan, R. Sundaraganapathy, and C. Jothimanivannan, Arab. J. Chem. 10 (2017) 928.

[2] V. S. Tambe, M. N. Deodhar, and V. Prakyacd, Bull. Fac. Pharm. Cairo Univ. 54 (2016) 87.

[3] P. Santhosh, N. S. Kumar, M. Renukadevi, A. I. Gopalan, T. Vasudevan, and K. P. Lee, Anal. Sci. 23 (2007) 475.

[4] T. S. Belal, D. S. El-Kafrawy, M. S. Mahrous, M. M. Abdel-Khalek, and A. H. Abo-Gharam, Ann. Pharm. Fr. 4 (2016) 267.

[5] J. D. Fegade, H. P. Mehta, R. Y. Chaudhari, and V. R. Patil, Int. J. Chem. Tech. Res. 1 (2009) 189.

[6] G. Sunil, M. Jambulingam, S. A. Thangadurai, D. Kamalakannan, R. Sundaraganapathy, and C. Jothimanivannan, Arabian J. Chem. 10 (2017) 928.

[7] P. D. Kalariya, D. Namdev, R. Srinivas, and S. Gananadhamua, J. Saudi Chem. Soc. 21 (2017) 373.

[8] R. S. Naeem, A. Muhammad, and I. I. M. Ullah akhanand, Quim. Nova. 1 (2011) 200.

[9] P. L. K. M. Rao, V. Venugopal, Ch. S.G. Teja, D. V. N. S. Radhika, K. Kavitha, S. Lavanya, T. Manasa, and A. Pavani, Int. J. Chem. Pharm. Chem. 1 (2011) 129.

[10] H. El-Desoky, M. Abdel-Galeil, and A. Khalifaa, J. Electroanal. Chem. 846 (2019) 113.

[11] S. K. Rupesh, D. K. Archana, P. G. Keshao, B. V. Bakad, M. A. Channawa, and A. V. Chandewar, Int. J. Chem. Pharm. Res. Dev. 2 (2010) 126.

[12] A. A. El-Masry, M. E. A. Hammoud, D. R. El-Wasseef, and S. M. El-Ashry, Spectrochim. Acta A 191 (2018) 413.

[13] T. Alizadeh, and L. Allahyari, Electrochim. Acta 111 (2013) 663.

[14] A. Afkhami, H. Ghaedi, T. Madrakian, M. Ahmadi, and H. Mahmood-kashani, Biosens. Bioelectron.44 (2013) 34.

[15] D. Kumar, and B. B. Prasad, Sens. Actuators B 171-172 (2012) 1141.

[16] X. Kan, H. Zhou, C. Li, A. Zhu, Z. Xing, and Z. Zhao, Electrochim. Acta 63 (2012) 69.

[17] M. B. Gholivand, M. Torkashvand, and Gh. Malekzadeh, Anal. Chim. Acta 713 (2012) 36.

[18] M. Cegłowski, and G. Schroeder, Compr. Anal. Chem. 86 (2019) 295.

[19] L. Zhao, F. Zhao, and B. Zeng, Sens. Actuators B 176 (2013) 818.

[20] S. G. Ge, M. Yan, X. L. Cheng, C. C. Zhang, J. H. Yu, P. N. Zhao, and W. Q. Gao, J. Pharm. Biomed. Anal. 52 (2010) 615.

[21] X. L. Sun, X. W. He, Y. K. Zhang, and L. X. Chen, Talanta 79 (2009) 926.

[22] J. Huang, X. Zhang, S. Liu, Q. Lin, X. He, X. Xing, W. Lian, and D. Tang, Sens. Actuators B 152 (2011) 292.

[23] L. Li, T. Xue-cai, Z. Dan-dan, W. Lin, L. Fu-hou, and H. Zai-yin, Chem. Res. Chin. Univ. 28 (2012) 410.
[24] P. Liu, X. Zhang, W. Xu, C. Guo, and S. Wang, Sens. Actuators B 163 (2012) 84.
[25] Y. Wang, Z. Zhang, V. Jain, J. Yi, S. Mueller, J. Sokolov, Z. Liu, K. Levon, B. Rigas, and M. H. Rafailovich, Sens. Actuators B 146 (2010) 381.
[26] B. B. Prasad, R. Madhuri, M. P. Tiwari, and P. S. Sharma, Biosens. Bioelectron. 25 (2010) 2140.
[27] J. Zhang, Y. Q. Wang, R. H. Lv, and L. Xu, Electrochim. Acta 55 (2010) 4039.
[28] B. B. Prasad, R. Madhuri, M. P. Tiwari, and P. S. Sharma, Talanta 81 (2010) 187.
[29] T. Alizadeh, and M. Akhoundian, Electrochim. Acta 55 (2010) 3477.
[30] A. Nezhadali, L. Mehri L, and R. Shadmehri, Sens. Actuators B 171-172 (2010) 1125.
[31] A. Nezhadali, and R. Shadmehri, Sens. Actuators B 177 (2013) 871.
[32] A. Nezhadali, S. Pirayesh, and R. Shadmehri, Sens. Actuators B 185 (2013) 17.
[33] A. Nezhadali, and M. Mojarrab, Sens. Actuators B 190 (2014) 829.
[34] L. Özcan, and Y. Şahin, Sens. Actuators B 127 (2007) 362.
[35] B. Li, Y. Zhou, W. Wu, M. Liu, S. Mei, Y. Zhou, and T. Jing, Biosens. Bioelectron. 67 (2015) 121.
[36] C. Xue, Q. Han, Y. Wang, J. Wu, T. Wen, R. Wang, J. Hong, X. Zhou, and H. Jiang, Biosens. Bioelectron. 49 (2013) 199.
[37] S. Hong, L. Yoon, S. Lee, M. H. So, and K. Y. Wong, Electroanalysis 25 (2013) 1085.
[38] V. V. Shumyantseva, T. V. Bulko, L. V. Sigolaeva, A. V. Kuzikov, and A. I. Archakov, Biosens. Bioelectron. 86 (2016) 330.
[39] C. Malitesta, M. R. Guascito, E. Mazzotta, and R. A. Picca, Thin Solid Films 518 (2010) 3705.
[40] S. Menon, S. Jesny, and K. G. Kumar, Talanta 179 (2018) 668.
[41] J. Li, J. Zhao, and X. Wei, Sens. Actuators B 140 (2009) 663.
[42] M. Pumera, Chem. Eur. J. 15 (2009) 4970.
[43] H. Beitollahi, H. Karimi-Maleh, and H. Khabazzadeh, Anal. Chem. 80 (2008) 9848.
[44] A. Benvidi, P. Kakoolaki, H. R. Zare, and R. Vafazadeh, Electrochim. Acta 56 (2011) 2045.
[45] R. T. Kachoosangi, M. M. Musameh, I. Abu-Yousef, J. M. Y. S. M. Kanan, L. Xiao, S. G. Davies, A. Russell and R. G. Compton, Anal. Chem. 81 (2009) 435.
[46] T. Wen, W. Zhu, C. Xue, J. Wu, Q. Han, X. Wang, X. Zhou, and H. Jiang, Biosens. Bioelectron. 56 (2014) 180.
[47] A. Nezhadali, and M. Mojarrab, Anal. Chim. Acta 924 (2016) 86.
[48] M. Riskin, R. Tel-Vered, T. Bourenko, E. Granot, and I. Willner, J. Am. Chem. Soc. 130 (2008) 9726.
[49] J. Wang, and M. Musameh, Anal. Chem. 75 (2003) 2075.

[50] S. Hrapovic, Y. Liu, K. B. Male, and J. H. T. Luong, Anal. Chem. 76 (2004) 1083.
[51] M. G. Zhang, A. Smith, and W. Gorski, Anal. Chem. 76 (2004) 5045.
[52] S. Kunath, N. Marchyk, K. Haupt, and K. H. Feller, Talanta 105 (2013) 211.
[53] O.W. Gooding, and C. Opin, Chem. Biol. 8 (2004) 297.
[54] B. B. Prasad, R. Madhuri, M. P. Tiwari, and P. S. Sharma, Electrochim. Acta 55 (2010) 9146.
[55] S. Sadeghi, A. Motaharian, and A. Zeraatkar Moghaddam, Sens. Actuators B 168 (2012) 336.
[56] C. R. T. Tarley, G. Silveira, W. N. L. Santos, G. D. Matos, E. G. P. Silva, M. A. Bezerra, M. Miró, and S. L. C. Ferreira, Microchem. J. 92 (2009) 58.
[57] A. Nezhadali, and M. Mojarrab, J. Electroanal. Chem. 744 (2015) 85.
[58] C. Long, L. Li, M. Zhai, and Y. Shan, J. Phys. Chem. Solids 134 (2019) 255.
[59] M. Roushani, A. Nezhadali, Z. Jalilian, and A. Azadbakht, Mater. Sci. Eng. C 71 (2017) 1106.
[60] K. Damodhar Reddy, K. Sayanna, and G. Venkateshwarlu, Int. J. Pharm. Sci. Res. 5 (2014) 2714.
[61] S. K. Dubey, J. Hemanth, C. Venkatesh, R. N. Saha, and S. Pasha, J. Pharm. Anal. 2 (2012) 462.
[62] R. M. Hanabaratti, J. I. Gowda, and S. M. Tuwar, Asian J. Pharm. Clin. Res. 12 (2019) 199.